



HAL
open science

Silver isotope and volatile trace element systematics in galena samples from the Iberian Peninsula and the quest for silver sources of Roman coinage

Jean Milot, Mariano Ayarzagüena Sanz, Chloé Malod-Dognin, Francis Albarède, Philippe Telouk, Janne Blichert-Toft

► To cite this version:

Jean Milot, Mariano Ayarzagüena Sanz, Chloé Malod-Dognin, Francis Albarède, Philippe Telouk, et al.. Silver isotope and volatile trace element systematics in galena samples from the Iberian Peninsula and the quest for silver sources of Roman coinage. *Geology*, 2021, 50 (4), pp.422-426. 10.1130/G49690.1 . hal-03616540

HAL Id: hal-03616540

<https://hal.science/hal-03616540v1>

Submitted on 22 Mar 2022

HAL is a multi-disciplinary open access archive for the deposit and dissemination of scientific research documents, whether they are published or not. The documents may come from teaching and research institutions in France or abroad, or from public or private research centers.

L'archive ouverte pluridisciplinaire **HAL**, est destinée au dépôt et à la diffusion de documents scientifiques de niveau recherche, publiés ou non, émanant des établissements d'enseignement et de recherche français ou étrangers, des laboratoires publics ou privés.

1 Ag isotope and volatile trace element systematics in galena samples
2 from the Iberian Peninsula and the quest for silver sources of Roman
3 coinage
4

5 Jean Milot^{1*}, Janne Blichert-Toft¹, Mariano Ayarzagüena Sanz², Chloé Malod-Dognin¹,
6 Philippe Télouk¹ and Francis Albarède¹

7 ¹ENS Lyon, CNRS, Université de Lyon, France

8 ²Sociedad Española de Historia de la Arqueología, 28350 Ciempozuelos (Madrid), Spain
9

10 Corresponding author: jean.milot@ens-lyon.fr
11

12 **Abstract**

13 Silver played a major role in the progressive monetization of antique Mediterranean. Here, we
14 combine Pb and Ag isotopes with volatile trace elements (Bi, Sb, As) to assess whether,
15 during the Roman occupation of Iberia, galena constituted a significant source of silver. We
16 find that Pb and Ag isotopic compositions of 47 samples of galena from eight different Iberian
17 mining provinces, many of them exploited during Roman times, are uncorrelated which
18 indicates that their respective isotopic variabilities depend on different petrogenetic processes.
19 Moreover, the range of Ag isotopic abundances is ~6 times wider than that displayed
20 worldwide by silver coins in general and Roman silver coins in particular. Although galena
21 from the Betics provide the best fit for Pb isotopes with Roman coins, their fit with Ag
22 isotopic compositions is at best sporadic. We suggest that, together with Sb, Bi, and As, silver
23 is primarily derived from fluids boiled off from differentiated mantle-derived magmas. These
24 fluids in turn reacted with pre-existing galena, acting as a silver trap. Lead sulfides with
25 $\epsilon^{109}\text{Ag} \sim 0$ and unusually rich in Ag, Sb, Bi, and As were the most probable sources of ancient
26 silver, whereas samples with $\epsilon^{109}\text{Ag}$ departing significantly from ~ 0 reflect low-temperature
27 isotopic fractionation processes in the upper crust.
28

29 **1. Introduction**

30 Considered a luxury commodity, silver has been massively used for coinage from the 7th
31 century BC onwards. It took monetized silver, which first appeared in the Aegean and
32 Anatolian regions, centuries to reach the Occidental Mediterranean. Argentiferous galena
33 (PbS) is considered by some as the main source of silver during ancient times (e.g. Domergue,
34 2008, 1990) with silver having been extracted from PbS by smelting and subsequent
35 cupellation in the presence of metallic lead (e.g. Pernicka et al., 1998; Tylecote, 1992). Others
36 suggest alternative Ag-rich minerals such as plumbojarosite, tetrahedrite, or chlorargyrite (e.g.
37 Anguilano et al., 2010). In general, whichever the sources of silver for Roman coinage, they
38 have since been used up and whatever is left is so dispersed that it is difficult to assess
39 whether they ever constituted major sources of bullion or were barren PbS.

40 In contrast to the relative abundances of radiogenic Pb isotopes, which vary with time and the
41 relative proportions of U, Th, and Pb in the ore source, Ag, Cu, and Zn isotopic abundances
42 vary with the nature of fluids and mineral phases contributing to the ore, redox conditions,
43 and the temperature of ore formation. Isotopic variations are related to mass-dependent
44 fractionation and are typically in the range of a fraction of a percent per atomic mass unit for
45 Cu and Zn and one per mil for Ag. Silver isotopic variations are most conveniently reported in
46 epsilon units ($\epsilon^{109}\text{Ag}$; the deviation per 10,000 of a given sample relative to the NIST 978a Ag
47 standard). For the entire body of antique coinage analyzed so far, this range is strikingly
48 narrow within only $\pm 1 \epsilon$ unit (Albarède et al., 2020, 2016; Desaulty et al., 2011; Desaulty and
49 Albarede, 2013). Since Ag, Cu, and Zn isotopic variations are controlled by thermodynamics
50 rather than geology, they are of marginal interest for provenance studies and rather track ore
51 genesis processes (Arribas et al., 2020).

52 A trademark of Ag isotopes particularly relevant to archeology is the contrast between the
53 narrow range of $\epsilon^{109}\text{Ag}$ ($< 2 \epsilon$ units) in silver coins of different origins and age of minting
54 (Ancient Greece and Rome; Medieval Europe; colonial South and Central Americas)
55 (Desaulty et al., 2011; Fujii and Albarède, 2018) and the 12 ϵ unit range measured in Ag and
56 Ag-bearing base metal (Pb, Zn, Cu) ores (Arribas et al., 2020). Iberia was the major source of
57 silver for the Carthaginian and Roman worlds up until the 2nd century AD and Pb isotope data
58 on potential silver ores are extremely well documented (see García de Madinabeitia et al.,
59 2021 and references therein). We therefore measured Ag isotopes and trace element
60 abundances on the galena sample suite documented for Pb isotopes by Milot et al. (2021a) to

61 identify which of these Iberian Pb ores may have actually been mined for use of their silver in
62 minting Roman *denarii*.

63

64 **2. Potential Iberian sources of Roman lead and silver**

65 Geological information on the galena samples analyzed here is summarized in Milot et al.
66 (2021a) and further details can be found in the IBERLID database (García de Madinabeitia et
67 al., 2021). Briefly, most deposits of economic importance are located in the southern part of
68 the Iberian Peninsula (see Supplementary Material). Lead-zinc-rich deposits occur
69 particularly in the Betic Cordillera (southeast Iberia), the Sierra Morena (south-central Iberia),
70 which belongs to the Central Iberian Zone (CIZ), and the Ossa Morena Zone (OMZ,
71 southwest of the Sierra Morena). The South Portuguese Zone (SPZ) counts many world-class
72 giant and supergiant volcanogenic massive sulfide (VMS) deposits all belonging to the
73 Iberian Pyrite Belt that covers the southwest corner of the Iberian Peninsula. Although less
74 common, notable deposits occur in the northern part of the Iberian Peninsula, such as in the
75 Catalanian Coastal Ranges, the Northern Iberian Massif, the Basque-Cantabrian Basin, the
76 Cantabrian Zone, and the West Asturian Leonese Zone (Fig. 1). These mining regions exhibit
77 archeological evidence of ancient exploitation from the Bronze Age to the Roman period.

78

79 **3. Materials and methods**

80 The Ag isotopic compositions and Ag, Sb, Bi, As, Pb, and Cu concentrations of 47 Iberian
81 galena samples are listed in Table SM1. Table SM2 lists the Pb isotopic compositions for
82 these same samples and samples from the literature. Samples were grouped into eleven
83 distinct regions (Fig. 1), which correspond to the different tectonostratigraphic units that form
84 the Iberian Peninsula (e.g. Vergés et al., 2019). For better readability, the Central Iberian
85 Zone to which the metallogenic province of the Sierra Morena belongs was divided into two
86 distinct mining areas, those of the Linares-La Carolina and Alcudia Valley-Los Pedroches
87 districts.

88 The Pb and Ag isotopic compositions of Roman silver coins discussed below are from the
89 literature (Albarède et al., 2020, 2016; Desaulty et al., 2011; Westner et al., 2020). The type
90 and age of these coins are reported in Table SM3 and date mainly from the 3rd and 2nd

91 centuries BC, with a few exceptions dating to the early 1st century BC. We established two
92 groups corresponding to coins minted before and after the Roman 211 BC monetary reform.

93 The analytical protocols for Ag separation and isotopic measurement are described in Milot et
94 al. (2021b), while the protocols used for measuring the concentrations of Ag, Sb, Bi, As, Pb,
95 and Cu are given in the Supplementary Material.

96

97 **4. Results**

98 The Ag isotope compositions of the present galena samples span a range of more than 10
99 $\epsilon^{109}\text{Ag}$ units (-8.05 to +2.27), consistent with the findings of Arribas et al. (2020), and vary
100 broadly within each region with significant overlap between regions. In stark contrast, $\epsilon^{109}\text{Ag}$
101 of Roman silver coins fall within a narrow range (-1.05 to +0.37) except for a single outlier
102 with heavier $\epsilon^{109}\text{Ag}$ of 1.32 ± 0.08 . No noticeable differences in Ag isotopic composition are
103 observed between Roman coins minted before and after the 211 BC monetary reform or for
104 three Carthaginian coins. Iberian galena samples match only sporadically the Ag isotopic
105 compositions of Roman coins: among the 47 samples analyzed, only six galena ores fall
106 within the range of the coins (one from the Eastern Betics, one from the Linares-La Carolina
107 district, two from the Alcuía Valley-Los Pedroches district, one from the Ossa Morena Zone,
108 and one from the South Portuguese Zone).

109 The extent of Ag isotopic variability displayed by galena samples from the Iberian Peninsula
110 is of the same order as the -4 to +4 $\epsilon^{109}\text{Ag}$ range exhibited by hypogene native silver (Arribas
111 et al., 2020; Mathur et al., 2018) but tends to be overall more negative (Fig. 2). $\epsilon^{109}\text{Ag} < -4$ is
112 common in Iberian galena samples, whereas they are rare in other primary or oxidized silver
113 minerals.

114 With a few exceptions, the log-log (Ag+Cu)/Pb vs Sb/Pb diagram shows a positive correlation
115 between these trace elements (Fig. 3a). Furthermore, both Sb vs $\epsilon^{109}\text{Ag}$ (Fig. 3b) and Ag vs
116 $\epsilon^{109}\text{Ag}$ (Fig. 3c) show that samples with the highest Sb and Ag contents (>4000 and >3000
117 ppm, respectively) have $\epsilon^{109}\text{Ag}$ values centered around about -1.5, only slightly lighter than
118 the $\epsilon^{109}\text{Ag}$ range for silver coins.

119

5. Discussion

Only few studies so far have investigated the mechanisms of Ag isotope fractionation (Arribas et al., 2020; Fujii and Albarede, 2018; Mathur et al., 2018). Sulfides and sulfosalts play a major role in reduced environments. Pb_2S_2 (galena) can form solid solutions with AgBiS_2 (matildite), AgSbS_2 (miargyrite), and AgAsS_2 (proustite) (Hackbarth and Petersen, 1984; Renock and Becker, 2011) and a strong correlation between Ag and Sb+Bi contents is commonly observed in argentiferous galena (George et al., 2015). These mutually soluble molecules can exsolve from galena upon cooling (Chutas et al., 2008) or, alternatively, upon metamorphic reheating and melting, and recrystallize as interstitial minerals observable in thin sections (Voudouris et al., 2008). Other minerals may contain large concentrations of silver, notably chlorides (chlorargyrite). Under low-temperature, oxidized conditions, jarosite ($\text{KFe}_3(\text{SO}_4)_2(\text{OH})_6$) and native Ag are important silver-bearing minerals. Arribas et al. (2020) proposed that the oxidation of primary Ag-sulfides under supergene weathering conditions preferentially releases isotopically heavy Ag, which in turn reprecipitates beneath the water table as secondary Ag phases of equally heavy Ag isotopic composition.

As far as silver sources are concerned, the two most crucial questions to emerge from the present work are:

1. Which of the samples analyzed here may have been active sources of monetized Roman silver?
2. Why is the worldwide range of $\epsilon^{109}\text{Ag}$ (-1 to +1; Fujii and Albarede, 2018), including Ancient Greece and Rome, Medieval Europe, and colonial South and Central Americas, so narrow in coins compared to the range of $\epsilon^{109}\text{Ag}$ in potential Ag ores which is nearly two orders of magnitude wider (Arribas et al., 2020; this work)?

The answer to the first question is that, overall, only very few Iberian galena ores fit the Ag isotope compositions of Roman silver coins. Because the sources of Iberian Pb and Ag used in the coinage process may have been disconnected, Pb isotopes unfortunately are of little use to help identify potential silver sources with precision. Answering the second question is more complicated because of two factors: (i) Ag–O bonds tend to concentrate the heavy isotope ^{109}Ag with respect to Ag–S and Ag–Cl bonds; (ii) increasing temperature tends to reduce isotope fractionation with $1/T^2$, where T is the absolute temperature.

The narrow range of $\epsilon^{109}\text{Ag}$ in Roman coins indicates that their silver source was primarily extracted at high temperatures, presumably from the mantle (Fujii and Albarede, 2018). High

152 temperature will suppress any isotopic fractionation between magmas and crystallizing
153 minerals. The similar ranges of $\epsilon^{109}\text{Ag}$ in minted silver extracted by smelting (Greece, Rome)
154 and the patio method (colonial Latin America; Desautly et al., 2011) do not support the idea
155 that the high temperatures of smelting reduced the range of $\epsilon^{109}\text{Ag}$. Petrologic evidence,
156 however, is inconsistent with Ag-rich sulfides, such as argentiferous galena and sulfosalts,
157 crystallizing at magmatic temperatures. Fluid inclusion studies (e.g. Arribas et al., 1995;
158 Voudouris et al., 2008) point to crystallization and exsolution of $\text{Ag}(\text{Bi},\text{Sb},\text{As})\text{S}_2$ minerals
159 from galena solid solutions at temperatures of 150-400°C. For tetrahedrite, Hackbarth and
160 Petersen (1984) used strongly curved Cu, Ag, As, and Sb trajectories to suggest that these
161 elements are enriched by fractional crystallization from hydrothermal solutions. These
162 trajectories can, however, be alternatively interpreted as mixing relationships between Ag-
163 poor galena and an $\text{Ag}(\text{Sb},\text{As})\text{S}_2$ end-member: the $\text{Cu}+\text{Ag}/\text{As}+\text{Sb}$ ratios used in Hackbarth
164 and Petersen's (1984) study being highly variable along the trajectories, mixing such end-
165 members results, by definition, in hyperbolae with very strong curvature.

166 Given the extreme volatility of Ag, As, and Sb, mixing can therefore be used as a model to
167 interpret the Ag isotope compositions in galena: interaction between Ag-poor sulfides, such as
168 galena and sulfosalts, and Ag-Bi-Sb-As-rich fluids boiled off from magmas is expected to be
169 particularly efficient at assimilating Ag from percolating fluids. Chutas et al.'s (2008) data on
170 mineral stability in the system $\text{PbS}-\text{AgSbS}_2$ (their Fig. 7) shows that above 200°C, galena
171 behaves as a 'silver sponge' with respect to Sb-rich fluids. George et al.'s (2015) strong
172 correlations (their Table 3) between Ag and Bi in galena makes the extrapolation of this
173 suggestion to Sb- and As-rich fluids relatively straightforward. Argentiferous galena would
174 form in the relatively broad temperature range of PbS stability (150-450°C) upon Ag+Sb
175 uptake from Ag-Sb-Bi-As-rich magmatic and hydrothermal fluids by pre-existing Pb ore
176 deposits. Silver-rich galena could form from either an early phase of the same mineralization
177 event or, alternatively, multi-stage mineralization. Modern magmatic environments with
178 fluids enriched in Ag, As, Sb, and Bi, which can be used as analogs for silver ores, are known,
179 notably from the PACMANUS hydrothermal field situated on Pual Ridge next to Papua New
180 Guinea, and exsolved from felsic volcanic rocks (Binns, 2006; Wohlgemuth-Ueberwasser et
181 al., 2015).

182 With few exceptions, the Ag and Sb contents of our samples are positively correlated (Fig. 3)
183 ($r=0.81$), which argues for silver enrichment of galena by coupled substitution of 2Pb^{2+} by
184 Cu/Ag^+ and $\text{As}/\text{Bi}/\text{Sb}^{3+}$ leading to the formation of a solid solution between Pb_2S_2 and

185 AgSbS₂ from which each phase may subsequently exsolve upon cooling (Chutas et al., 2008;
186 George et al., 2015; Renock and Becker, 2011) (Fig. 4). Moreover, samples with the highest
187 Ag contents, which may have been of economic interest to Roman smelters, have a narrow
188 range of $\epsilon^{109}\text{Ag}$ centered at about $-1.5 \epsilon^{109}\text{Ag}$, which is included in the range of ore-forming
189 fluid compositions determined by Arribas et al. (2020) but slightly lighter than that of silver
190 coins. The lighter $\epsilon^{109}\text{Ag}$ values of Ag-rich galena may be explained by leaching of
191 preexisting fractionated Ag-rich deposits by Bi-Sb-As-rich hydrothermal fluids boiled off
192 from mantle-derived magma. Silver isotopic fractionation during partial exsolution of Ag
193 sulfides or sulfosalts from galena solid solutions may also be an explanation. Even slightly
194 fractionated from the mantle value of $\epsilon^{109}\text{Ag}\sim 0$, the Ag isotopic composition of Ag-rich
195 galena is likely to get averaged out in silver bullion during smelting. The Betics, where
196 Neogene magmatism took place (e.g. Arribas and Tosdal, 1994), is a plausible source of such
197 Ag-enriched ores as attested to by archeological evidence (Baron et al., 2017; Domergue,
198 2008, 1990). Similarly, in other provinces, hydrothermal fluids of magmatic origin most
199 likely are responsible for the Ag enrichment of lead ores, which may have been important
200 sources of silver for ancient miners. Since the Pb isotope compositions of the silver coins
201 considered here range between those of two lead sources from the Eastern Betics (Fig. SM1),
202 we suggest that Pb ore deposits from this province mostly were exploited for Pb in general
203 and cupellation in particular.

204 In contrast, silver from Ag-poor samples is isotopically fractionated relative to a given
205 reference value which, pending proper isotopic documentation, could be that of the mantle or
206 the crust and hence rather reflects supergene Ag fractionation processes in upper crustal
207 environments. Their $\epsilon^{109}\text{Ag}$ values differ markedly from those of Roman silver coins.

208

209 **6. Acknowledgments**

210 This work is a contribution of Advanced Grant 741454-SILVER-ERC-2016-ADG ‘Silver
211 Isotopes and the Rise of Money’ awarded to FA by the European Research Council. We are
212 grateful to those who contributed samples to the present study and spared time for their
213 careful selection: Eloïse Gaillou (Mineralogy Museum, MINES ParisTech), Ramón Jiménez
214 Martínez (Instituto Geológico y Minero de España), and Paul W. Pohwat and Elizabeth
215 Cottrell (Smithsonian Institution). Insightful reviews by Sonia Garcia de Madinabeitia,
216 Antonia Arribas, and an anonymous reviewer are gratefully acknowledged.

217

218 **7. References cited**

- 219 Albarède, F., Blichert-Toft, J., Callataÿ, F., Davis, G., Debernardi, P., Gentelli, L., Gitler, H.,
220 Kemmers, F., Klein, S., Malod-Dognin, C., Milot, J., Télouk, P., Vaxevanopoulos, M.,
221 Westner, K., 2020. From commodity to money: the rise of silver coinage around the
222 ancient Mediterranean (6th -1st century BCE). *Archaeometry* arcm.12615.
223 <https://doi.org/10.1111/arcm.12615>
- 224 Albarède, F., Blichert-Toft, J., Rivoal, M., Telouk, P., 2016. A glimpse into the Roman
225 finances of the Second Punic War through silver isotopes. *Geochem. Persp. Let.* 127–
226 137. <https://doi.org/10.7185/geochemlet.1613>
- 227 Anguilano, L., Rehren, T., Müller, W., Rothenberg, B., 2010. The importance of lead in the
228 silver production at Riotinto (Spain): L'importance du plomb dans la production
229 d'argent à Riotinto (Espagne). *archeosciences* 269–276.
230 <https://doi.org/10.4000/archeosciences.2833>
- 231 Arribas, A., Cunningham, C.G., Rytuba, J.J., Rye, R.O., Kelly, W.C., Podwysocki, M.H.,
232 McKee, E.H., Tosdal, R.M., 1995. Geology, geochronology, fluid inclusions, and
233 isotope geochemistry of the Rodalquilar gold alunite deposit, Spain. *Economic*
234 *Geology* 90, 795–822. <https://doi.org/10.2113/gsecongeo.90.4.795>
- 235 Arribas, A., Mathur, R., Megaw, P., Arribas, I., 2020. The Isotopic Composition of Silver in
236 Ore Minerals. *Geochemistry, Geophysics, Geosystems* 21, e2020GC009097.
237 <https://doi.org/10.1029/2020GC009097>
- 238 Arribas, A., Tosdal, R.M., 1994. Isotopic composition of Pb in ore-deposits of the Betic
239 Cordillera, Spain - Origin and relationship to other European deposits. *Economic*
240 *Geology* 89, 1074–1093. <https://doi.org/10.2113/gsecongeo.89.5.1074>
- 241 Baron, S., Rico, C., Antolinos Marín, J.A., 2017. Le complexe d'ateliers du Cabezo del Pino
242 (Sierra Minera de Cartagena-La Unión, Murcia) et l'organisation de l'activité minière
243 à Carthago Noua à la fin de la République romaine. Apports croisés de l'archéologie et
244 de la géochimie. *Arch. esp. arqueol.* 90, 147.
245 <https://doi.org/10.3989/aespa.090.017.007>
- 246 Binns, R.A., 2006. Data Report: Geochemistry of Massive and Semimassive Sulfides from
247 Site 1189, Ocean Drilling Program Leg 193, in: Barriga, F.J.A.S., Binns, R.A., Miller,
248 D.J., and Herzig, P.M. (Eds.), *Proc. ODP, Sci. Results*, 193, 1–22.
- 249 Chutas, N.I., Kress, V.C., Ghiorso, M.S., Sack, R.O., 2008. A solution model for high-
250 temperature PbS-AgSbS₂-AgBiS₂ galena. *American Mineralogist* 93, 1630–1640.
251 <https://doi.org/10.2138/am.2008.2695>

- 252 Garcia de Madinabeitia, S., Ibarguchi, J. G., & Zalduegui, J. S., 2021. IBERLID: A lead
253 isotope database and tool for metal provenance and ore deposits research. *Ore*
254 *Geology Reviews*, 104279. <https://doi.org/10.1016/j.oregeorev.2021.104279>
- 255 Desaulty, A.-M., Albarede, F., 2013. Copper, lead, and silver isotopes solve a major
256 economic conundrum of Tudor and early Stuart Europe. *Geology* 41, 135–138.
257 <https://doi.org/10.1130/G33555.1>
- 258 Desaulty, A.M., Telouk, P., Albalat, E., Albarede, F., 2011. Isotopic Ag-Cu-Pb record of
259 silver circulation through 16th-18th century Spain. *Proceedings of the National*
260 *Academy of Sciences of the United States of America* 108, 9002–9007.
261 <https://doi.org/10.1073/pnas.1018210108>
- 262 Domergue, C., 2008. *Les Mines Antiques. La Production des Métaux aux Epoques Grecques*
263 *et Romaines*. Picard, Paris.
- 264 Domergue, C., 1990. *Les mines de la Péninsule Ibérique dans l'antiquité romaine*,
265 *Publications de l'École française de Rome*.
- 266 Fujii, T., Albarede, F., 2018. 109Ag–107Ag fractionation in fluids with applications to ore
267 deposits, archeometry, and cosmochemistry. *Geochimica et Cosmochimica Acta* 234,
268 37–49. <https://doi.org/10.1016/j.gca.2018.05.013>
- 269 George, L., Cook, N.J., Cristiana, L., Wade, B.P., 2015. Trace and minor elements in galena:
270 A reconnaissance LA-ICP-MS study. *American Mineralogist* 100, 548–569.
271 <https://dx.doi.org/10.2138/am-2015-4862>
- 272 Hackbarth, C.J., Petersen, U., 1984. A fractional crystallization model for the deposition of
273 argentian tetrahedrite. *Economic Geology* 79, 448–460.
274 <https://doi.org/10.2113/gsecongeo.79.3.448>
- 275 Mathur, R., Arribas, A., Megaw, P., Wilson, M., Stroup, S., Meyer-Arrivillaga, D., Arribas, I.,
276 2018. Fractionation of silver isotopes in native silver explained by redox reactions.
277 *Geochimica et Cosmochimica Acta* 224, 313–326.
278 <https://doi.org/10.1016/j.gca.2018.01.011>
- 279 Milot, J., Blichert-Toft, J., Ayarzagüena Sanz, M., Fetter, N., Télouk, P., Albarède, F., 2021a.
280 The significance of galena Pb model ages and the formation of large Pb-Zn
281 sedimentary deposits. *Chemical Geology* 583, 120444.
282 <https://doi.org/10.1016/j.chemgeo.2021.120444>
- 283 Milot, J., Malod-Dognin, C., Blichert-Toft, J., Télouk, P., Albarède, F., 2021b. Sampling and
284 combined Pb and Ag isotopic analysis of ancient silver coins and ores. *Chemical*
285 *Geology* 564, 120028. <https://doi.org/10.1016/j.chemgeo.2020.120028>
- 286 Pernicka, E., Rehren, T., Schmitt-Strecker, S., 1998. Late Uruk silver production by
287 cupellation at Habuba Kabira, Syria. *Metallurgica Antiqua, der Anschnitt* 8, 123–134.

- 288 Renock, D., Becker, U., 2011. A first principles study of coupled substitution in galena. *Ore*
 289 *Geology Reviews* 42, 71–83. <https://doi.org/10.1016/j.oregeorev.2011.04.001>
- 290 Tylecote, R.F., 1992. *A history of metallurgy*. Maney Publishing.
- 291 Vergés, J., Kullberg, J.C., Casas-Sainz, A., de Vicente, G., Duarte, L.V., Fernández, M.,
 292 Gómez, J.J., Gómez-Pugnaire, M.T., Sánchez, A.J., López-Gómez, J., 2019. An
 293 introduction to the Alpine cycle in Iberia, in: *The Geology of Iberia: A Geodynamic*
 294 *Approach*. Springer, pp. 1–14.
- 295 Voudouris, P., Melfos, V., Spry, P., Bonsall, T.A., Tarkian, M., Solomos, C., 2008.
 296 Carbonate-replacement Pb–Zn–Ag±Au mineralization in the Kamariza area, Lavrion,
 297 Greece: Mineralogy and thermochemical conditions of formation. *Mineralogy and*
 298 *Petrology* 94, 85–106. <https://doi.org/10.1007/s00710-008-0007-4>
- 299 Westner, K.J., Birch, T., Kemmers, F., Klein, S., Höfer, H.E., Seitz, H. -M., 2020. ROME’S
 300 Rise to Power. Geochemical Analysis of Silver Coinage from the Western
 301 Mediterranean (Fourth to Second Centuries BCE). *Archaeometry* 62, 577–592.
 302 <https://doi.org/10.1111/arc.12547>
- 303 Wohlgemuth-Ueberwasser, C.C., Viljoen, F., Petersen, S., Vorster, C., 2015. Distribution and
 304 solubility limits of trace elements in hydrothermal black smoker sulfides: An in-situ
 305 LA-ICP-MS study. *Geochimica et Cosmochimica Acta* 159, 16–41.
 306 <https://doi.org/10.1016/j.gca.2015.03.020>

307

308 **Figure captions**

309 Figure 1. Map of the Iberian mining provinces and galena samples analyzed in this study.
 310 Circles: samples from this study (Table SM1); triangles: samples from the literature (Table
 311 SM2).

312 Figure 2. $\epsilon^{109}\text{Ag}$ of silver coins (Table SM3) and Iberian galena samples (Table SM1). Dotted
 313 lines delimit the range of Ag isotopic variation of silver coins, with the exception of one
 314 outlier.

315 Figure 3. (a) $(\text{Ag}+\text{Cu})/\text{Pb}$ vs Sb/Pb of Iberian galena samples in atomic concentration. The red
 316 line corresponds to a linear regression with a slope of 1. Note the logarithmic scale. (b) Sb vs
 317 $\epsilon^{109}\text{Ag}$ and (c) Ag vs $\epsilon^{109}\text{Ag}$ of Iberian galena samples. Dotted lines delimit the range of Ag
 318 isotopic variation of silver coins, with the exception of one outlier. The elemental
 319 concentrations are reported in Table SM1.

320 Figure 4. Solubility relationships in the PbS-AgSbS₂ system (after Chutas et al., 2008). gn =
321 galena; gn_{ss} = galena solid solution; fre = freieslebenite; mia = miargyrite. Silver sulfo-
322 antimonides are remarkably soluble in galena over a large range of temperatures. Galena
323 deposits represent an efficient trap for Ag-Sb rich fluids.

Figure 1

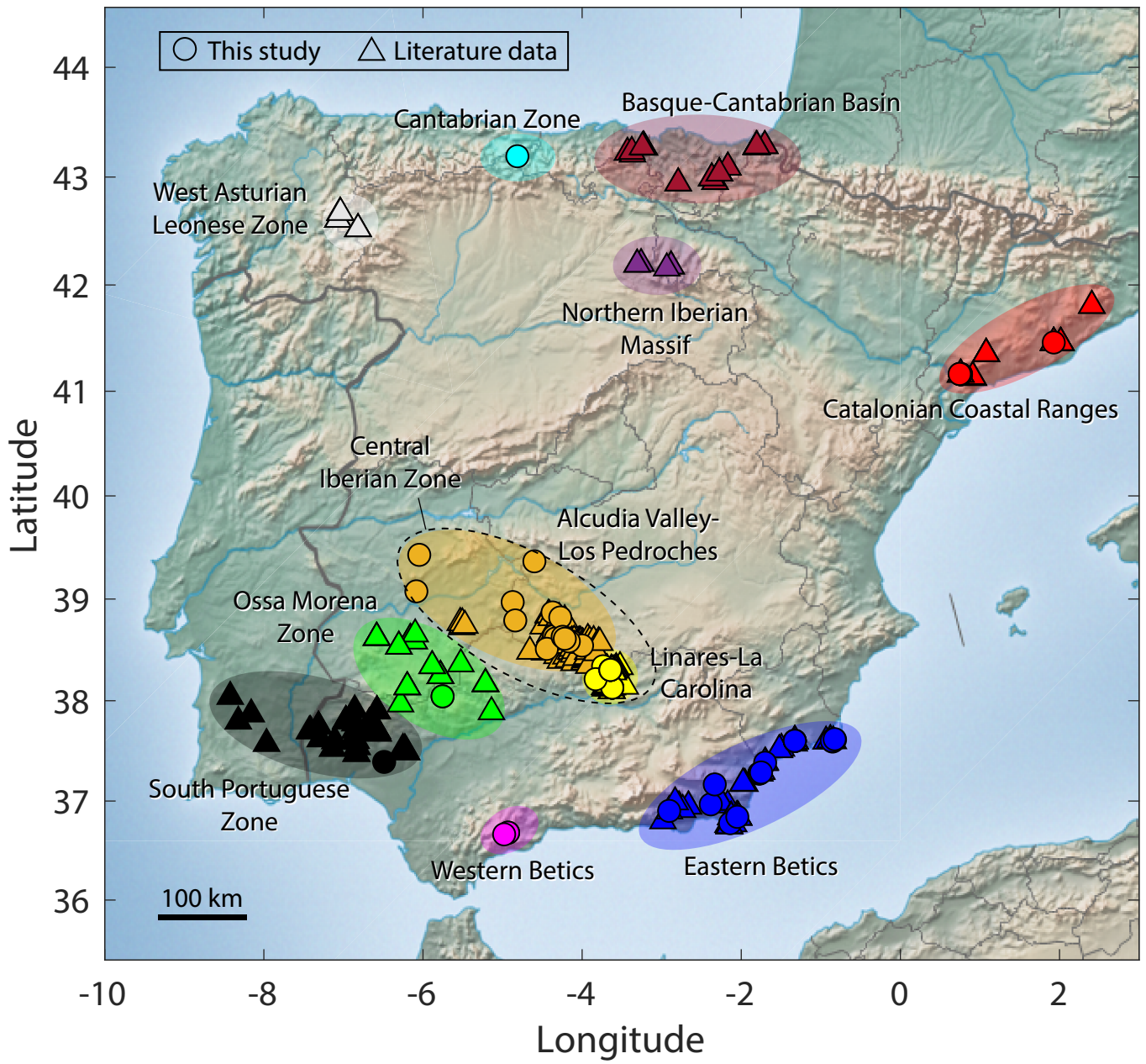


Figure 2

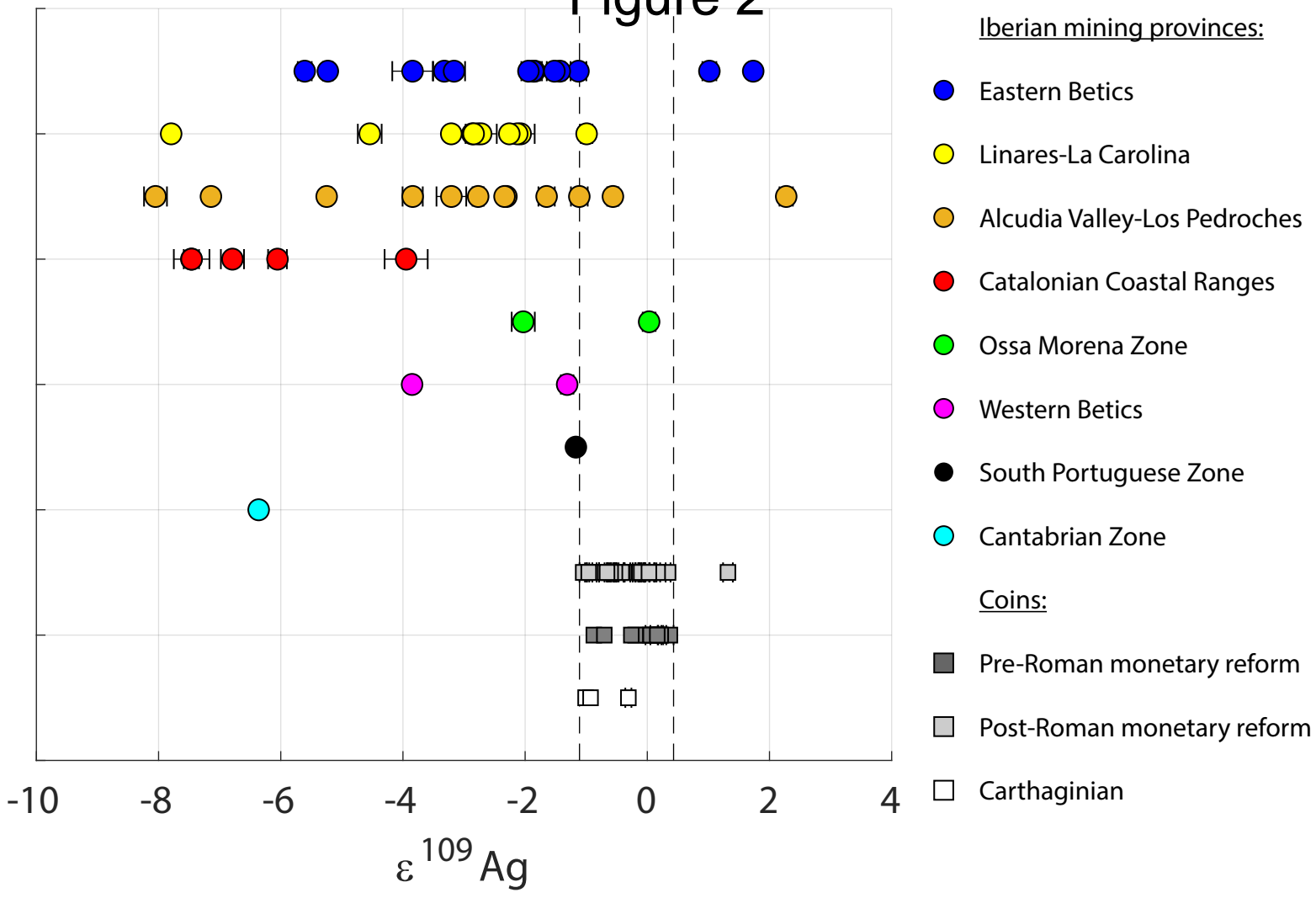
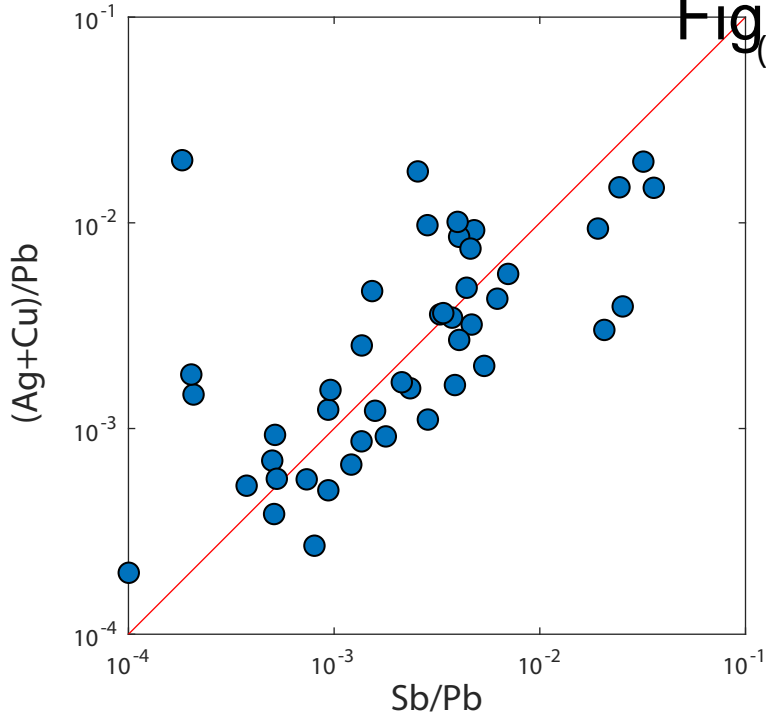


Figure 3



- Whole galena samples (a)
- Iberian mining provinces (b and c):
- Eastern Betics
- Linares-La Carolina
- Alcudia Valley-Los Pedroches
- Catalanian Coastal Ranges
- Ossa Morena Zone
- Western Betics
- South Portuguese Zone
- Cantabrian Zone

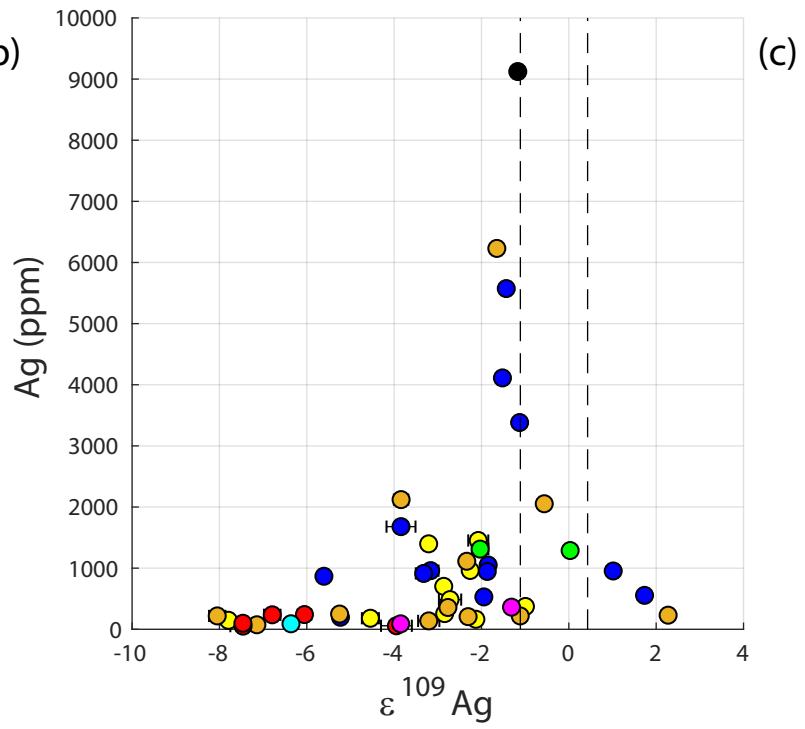
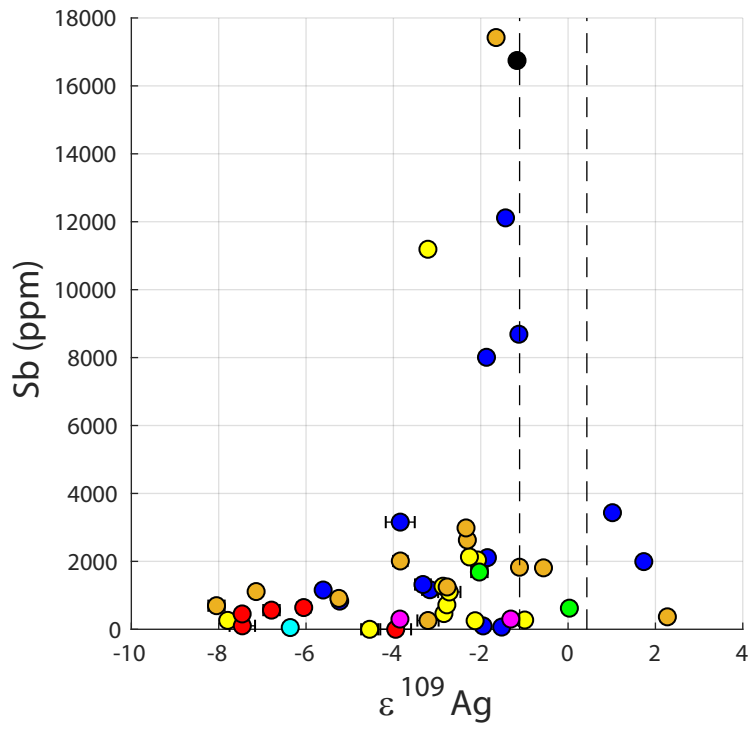
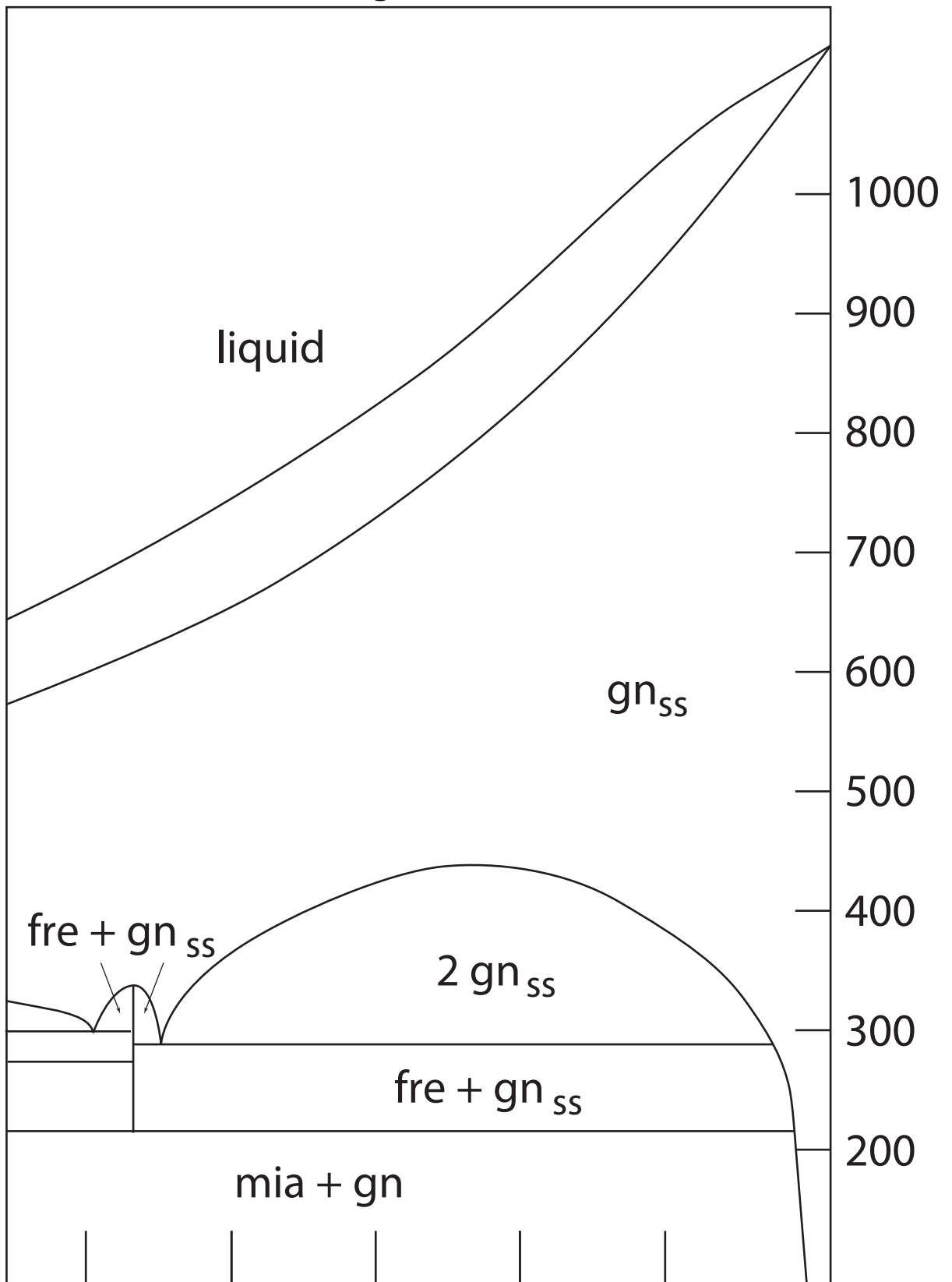


Figure 4

Temperature °C



50

40

30

20

10

Mole% fraction AgSbS₂